

Strange metal transport from coupling to fluctuating spins

Simone Fratini^{1*}, Arnaud Ralko¹, Sergio Ciuchi²

¹Université Grenoble Alpes, CNRS, Grenoble INP, Institut Néel, 38000 Grenoble, France.

²Dipartimento di Scienze Fisiche e Chimiche, Università dell'Aquila, Coppito-L'Aquila, Italy.

*Corresponding author. Email: simone.fratini@neel.cnrs.fr

Metals hosting strong electronic interactions, including high-temperature superconductors, behave in ways that do not conform to the normal Fermi liquid theory. To pinpoint the microscopic origin of this "strange metal" behavior, here we reexamine the transport and optical properties of the two-dimensional t-J model taking advantage of recent improvements made on the finite temperature Lanczos method (FTLM), enabling numerically exact calculations at unprecedentedly low temperatures and high spectral resolution. We find that strange metallicity is pervasive in the temperature-doping phase diagram wherever magnetic order is suppressed: it is driven by the presence of a fluctuating spin background, and it is therefore independent on hole concentration and unrelated to quantum criticality. Our results point to a two-step transport mechanism, with short- and long-time processes associated respectively with the charge and spin dynamics, the latter being responsible for both the strange metal character and the unconventional optical conductivities seen in experiments.

Strongly correlated materials often exhibit resistivities that increase linearly with temperature from few to hundreds of degrees K, at odds with the standard theory of metals (*I*). These anomalies are part of a broader, puzzling picture, as they also extend to the frequency domain: associated with

the strange behavior of charge transport, the decay of the conductivity with frequency is slower than predicted by exponential relaxation processes, and therefore incompatible with normal diffusion at long times (2).

Despite broad experimental evidence of the phenomenon, accurate numerical calculations of strange metal transport in correlated electron systems have only become available in the last decade. These have mostly focused either on the Hubbard model (3–8), due to its direct microscopic connection with the experimental systems, or to more phenomenology-driven descriptions enforcing the absence of quasiparticles and the concept of self-generated randomness, such as the SYK model and its generalizations (9), for their ability to capture the observed physical behavior.

Here we choose instead to work with the t-J model. Being itself derived from the Hubbard model — of which it constitutes the strong interaction limit, $U \rightarrow \infty$ — the t-J model retains a direct connection with the materials’ microscopics. However, the fact that charge fluctuations are mostly quenched when $U \rightarrow \infty$ strongly suppresses quasiparticles from the outset, hence establishing a conceptual link to SYK-type approaches. Importantly, it constitutes an ideal framework to disentangle the role of spin fluctuations from the many-body effects related to the charge: unlike in the Hubbard model, here the doping p sets the effective number of carriers independently on temperature, and the strength of magnetic correlations can be tuned independently of the correlation strength. Our results demonstrate strange metal behavior arising from the coupling of the hole carriers with the fluctuating spin environment, unrelated to quantum criticality, and shed light on the complex microscopic processes underlying the phenomenon.

Model and method.— The t-J model Hamiltonian is $H = - \sum_{ijs} t_{ij} (\tilde{c}_{is}^\dagger \tilde{c}_{js} + h.c.) + J_{ij} (\vec{S}_i \cdot \vec{S}_j - \frac{1}{4} n_i n_j)$, where \tilde{c}_{is}^\dagger and \tilde{c}_{js} are projected creation and annihilation operators for electrons on sites i and j , that take into account the constraint of no local double occupancy enforced by the strong Coulomb repulsion limit, n_i is the density at site i and J_{ij} is an antiferromagnetic (AF) exchange coupling between the corresponding quantum electron spins \vec{S}_i and \vec{S}_j . We focus on the square lattice, setting $t_{ij} = t$ and $J_{ij} = J$ for nearest neighbors (we take t as the energy unit). We also consider frustrated cases with $t_{ij} = t'$ and $J_{ij} = J'$ for next nearest neighbors.

We solve the t-J model numerically using the finite-temperature Lanczos method (FTLM) (10), supplemented by twisted boundary condition (TBC) averaging and a recently benchmarked

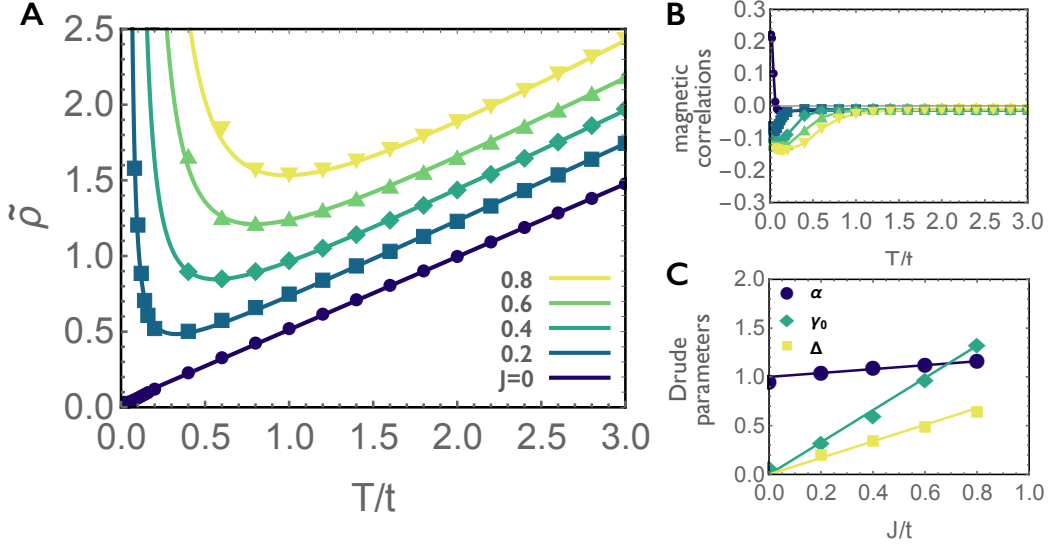


Figure 1: Strange metal behavior in the t-J model. (A) Resistivity per hole on the square lattice at different values of the AF exchange coupling (labels). The lines are fits through $\rho = \rho_0 e^{\Delta/T} + AT$, highlighting thermally activated behavior. Simulation parameters are $N_s = 18$, with $M = 1200$ pseudo-eigenstates and averaged over $N_\phi = 121$ TBC. For layered two-dimensional materials with interlayer separation d , physical units are restored upon multiplying the dimensionless resistivity by $\bar{\rho} = \hbar/e^2(d/x)$ for a concentration x of independent holes. (B) Spin correlations $\langle \vec{S}_i \cdot \vec{S}_j \rangle$ between a site i adjacent to the hole and j at the maximum allowed distance on the opposite sublattice. Antiferromagnetic correlations arise at $T \lesssim J$ except for $J = 0$, where Nagaoka ferromagnetism is established at very low temperatures. (C) Drude parameters and thermal activation energy, showing Planckian behavior with $\alpha \simeq 1$, $\gamma_0 \simeq 1.6J$ and $\Delta \simeq 0.85J$ (lines).

prescription for a reliable extrapolation of the Kubo formula to the d.c. limit (11). Taken together, these allow to reach high spectral resolution and unprecedentedly low temperatures, granting access to the experimentally relevant low temperatures and low frequencies (details in the supplement).

Strange metal behavior.— We first present our results for one hole in an unfrustrated square lattice. We will show later, and this is a key result of our study, that the scattering processes revealed here remain essentially unchanged at finite hole concentrations. Fig. 1A reports the dimensionless resistivity per hole, $\tilde{\rho}$, for different values of the antiferromagnetic exchange interaction J . Remarkably, the resistivity in the paramagnetic phase at $J = 0$ is linear in T from the highest down to the

lowest accessible temperature, here $T = 0.02t$.

Whether or not this applies to strange metals (12), we now analyze this result using the phenomenological Drude model, $\rho = m/(ne^2\tau)$ (13, 14), i.e. following the same procedure that is customarily used in experiments. In this framework, with the band mass m and the carrier density n given, the transport properties are entirely encoded in the transport scattering time τ . Using $m = \hbar^2/(2ta^2)$ for the square lattice, and taking n as the hole density, the transport scattering time can be extracted from the data as $\hbar/\tau = 2t\tilde{\rho}$.

Strange metals are *defined* by the linear relation

$$\hbar/\tau = \alpha k_B T + \gamma_0, \quad (1)$$

with γ_0 a constant: the T -linear behavior of the resistivity is ascribed to an equivalently T -linear dependence of the relaxation rate extracted from the Drude formula. When the numerical prefactor α is of order 1, the relaxation is termed Planckian (13–16). The slope extracted from the data in Fig. 1A for $J = 0$ is $\alpha = 0.94$ (see also panel B): the paramagnetic state of the t-J model (or, the Hubbard model in the $U \rightarrow \infty$ limit) is a Planckian metal at all temperatures.

The effect of a finite antiferromagnetic (AF) exchange coupling, $J > 0$, is also depicted in Fig. 1A. AF correlations build up upon lowering the temperature (shown in Fig. 1B) until the system orders antiferromagnetically at $T = 0$ (17–19), resulting in insulating behavior at low temperatures. A T -linear resistivity is recovered at all $T \gtrsim J$, as soon as the AF correlations vanish (cf. Fig. 1B). The recovery of uncorrelated spin dynamics is also indicated by the entropy approaching the value $k_B \log 2$ per spin (see supplement). From the Drude analysis, for all finite J we obtain the same Planckian slope $\alpha \simeq 1$ and a residual scattering rate $\gamma_0 \propto J$.

Optical conductivity and time-resolved carrier dynamics.— Despite being widely used as a useful phenomenological framework, the normal Drude description does not strictly apply to strange metals (12). This is because a Drude-like resistivity implies — and cannot be separated from — a Lorentzian form of the optical conductivity, $\sigma(\omega) = (1/\rho)/(1 + (\omega\tau)^2)$ (22), corresponding to an exponential decay of the current correlations with time. This simple form is generally not observed in experiments (2): strange metals typically exhibit instead a much slower power-law decay of the optical absorption at low frequencies, $\sigma(\omega) \sim \omega^{-c}$ with $c \lesssim 1$ (2, 23–26), making the identification of \hbar/τ with normal exponential relaxation processes debatable.

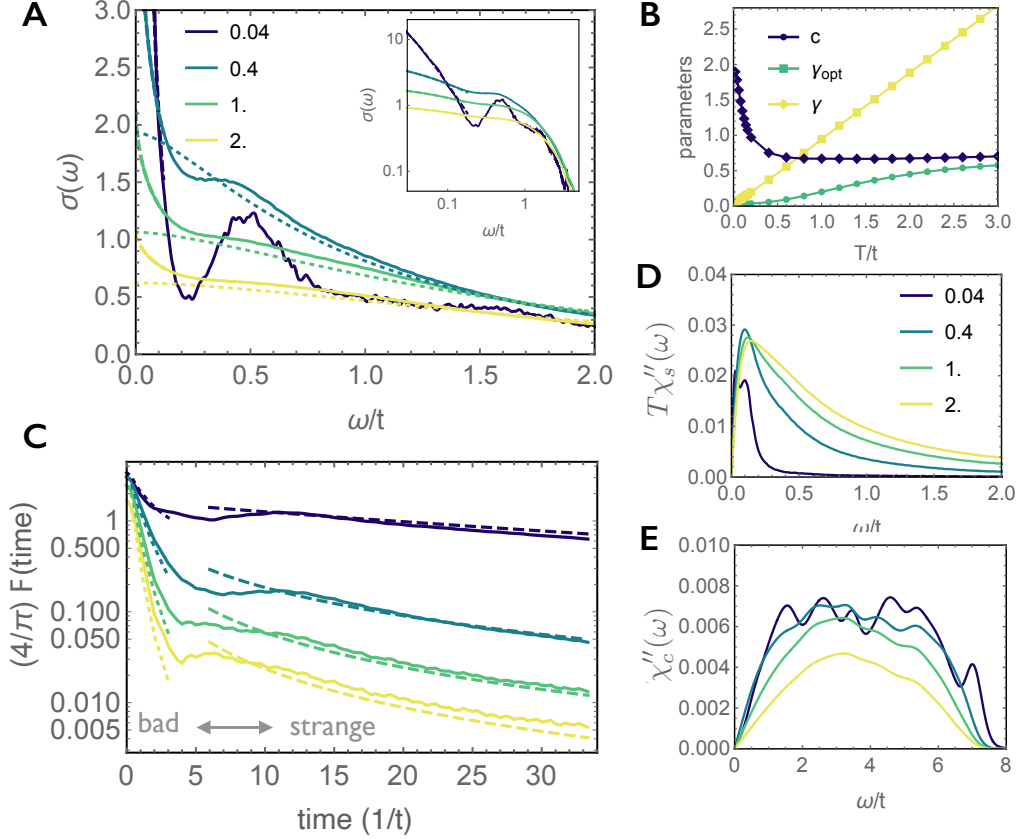


Figure 2: Optical conductivity and time-resolved dynamics. (A) Optical conductivity for the case $J = 0$ at different temperatures (legends). The dashed lines are fits to the low-frequency part of the optical conductivity via the stretched Drude ansatz $\sigma(\omega) = \sigma_0/(1 + (\omega\tau_{opt})^c)$, almost indistinguishable from the numerical data. The dotted lines are the RPA result from Ref. (20). The inset shows the same data in logarithmic scale. (B) Extracted exponent c together with the optical scattering rate $\gamma_{opt} = \hbar/\tau_{opt}$ and the transport scattering rate $\gamma = \hbar/\tau$. The optical scattering rate is always much lower than the transport scattering rate extracted via the Drude formula: this is a common feature in strongly interacting systems, reflecting the presence of considerable spectral weight at high energies (21). (C) Fourier transform of the optical conductivity. The dotted and dashed lines are Fourier transforms of the RPA optical conductivity and of the stretched Drude fits, respectively. (D) Local spin and (E) charge fluctuation spectrum calculated for different values of T/t .

Our optical conductivity data, shown in Fig. 2A, reproduce the behavior seen in experiments. We find that the low-frequency spectra accurately follow a "stretched" Drude form

$$\sigma(\omega) = \sigma_0 / (1 + (\omega\tau_{opt})^c), \quad (2)$$

shown as dashed lines. The anomalous exponent saturates to $c \simeq 2/3$ in the spin disordered phase at $J = 0$ (Fig. 2B), which is comparable with the exponent that is commonly observed in the cuprates (1, 2, 23), and incompatible with Drude-like relaxation. Exponents $2/3 \lesssim c \lesssim 1$ are also found in the presence of a finite J whenever AF correlations are suppressed (Fig. and Ref. (27)). Normal Drude behavior is only recovered in a narrow low-temperature regime at $J = 0$, where spin scattering is suppressed by the onset of the ferromagnetic Nagaoka state (28) (Fig. 2B).

Our numerical results substantiate the analysis performed in Refs. (24, 27), where a power-law dependence $\sigma(\omega) \sim 1/\omega^c$ with exponent $c \lesssim 1$ was obtained assuming a linear frequency dependence of the quasiparticle scattering rate, $\gamma(\omega) \propto \omega$, the latter being the defining feature of marginal Fermi liquids (also found in the t-J model (29)). The stretched Drude formula Eq. (2), however, does more than this: it shows that the complex non-Drude shape of the optical absorption observed in many correlated metals (1, 2, 23, 30) and that has traditionally required either a frequency-dependent scattering rate, in the so-called "extended Drude analysis", or the assumption of additional absorption channels in the alternative "two-fluid", "multi-component" or "Drude-Lorentz" analyses (31), follows entirely from one single parameter, c , that controls the form of the current relaxation.

The analytical form Eq. (2) is, at least, a useful tool for the analysis of optical absorption experiments. But what does such an anomalous frequency dependence of the optical absorption imply for the charge carrier dynamics? To answer this question, Fig. 2C shows the Fourier transform of the optical conductivity to the time domain, $F(t) = \int \sigma(\omega) \cos(\omega t) d\omega$. This quantity embodies the decay of the carrier velocity correlations resulting from collision events (22).

Not surprisingly, the time dynamics inferred from our data is much more complex than the simple exponential relaxation implied by the Drude model. The $F(t)$ traces show an initial sharp drop followed by a much slower relaxation at long times. The initial drop entails an almost complete loss of velocity correlations. It originates from the extremely broad optical absorption spectrum on the scale of the bandwidth itself, which is responsible for the "bad" metallic character of charge

transport (32–34). Notably, the high-frequency spectrum and the related short-time decay are well captured by local theories such as the retracable path approximation (20, 35) (RPA, dotted lines in panels A and C) or the analogous dynamical mean-field theory (DMFT) (36) (dotted lines).

More interesting to our purposes is the long time behavior, that is instead associated with the anomalous low-frequency response. The latter features a much slower relaxation resembling a stretched exponential (dashed lines). Because the transport properties are ultimately determined by the relaxation in the long-time limit, it follows that this feature is the one that carries the strange metal character.

The long-time relaxation processes revealed here suggest the emergence of an additional conduction channel rather than an additional source of scattering: the conductivity increases as compared to local approximations such as RPA and DMFT (low-frequency upturn in Fig. 2A); correspondingly, the $\rho \propto \sqrt{T}$ behavior characterizing these local theories transforms into the observed $\rho \propto T$ (supplement, Fig.). Our results indicate that the time needed to rearrange the spin environment in order to develop such additional conduction pathways is considerably longer than the timescale of individual hops (here the stretched relaxation appears at times $\sim 10/t$), highlighting their collective nature (37, 38). The fact that non-local processes increase the conductivity agrees with what has been reported in the Hubbard model (6, 39). We stress that the two-step relaxation demonstrated here at $J = 0$ is not restricted to this limit: Fig. in the Supplement shows similar time-dynamics in the quantum paramagnetic state obtained at finite J and finite t' (see below).

Spin and charge fluctuations.— To get more insights into the microscopic origin of this complex transport behavior, we show in Fig. 2D-E the imaginary part of the momentum-integrated spin $\chi_s''(\omega)$ and charge susceptibility $\chi_c''(\omega)$. The spin response has an overdamped oscillator shape that peaks at a low frequency $\omega_s \simeq t/10$, implying that the spin fluctuations are slow on the scale of the carrier hopping time. It obeys the functional form $\chi_s'' \propto \omega/(\omega^2 + \Gamma^2)$, that has been observed previously both in the pristine t-J model (40) and in its random J /random t generalization (41), and experimentally in the cuprates (42, 43). On the other hand, the charge fluctuation spectrum is much broader and featureless, extending on the scale of the bandwidth itself (here $8t$), also reminiscent of the charge response measured in the cuprates (44, 45).

Notably, the spin and charge timescales inferred from their respective fluctuation spectra co-

incide with the long and short-time processes observed in the current correlations in Fig. 2B. An analogous separation between spin and charge-related dynamics has been reported in the t - J_z model in Ref. (38).

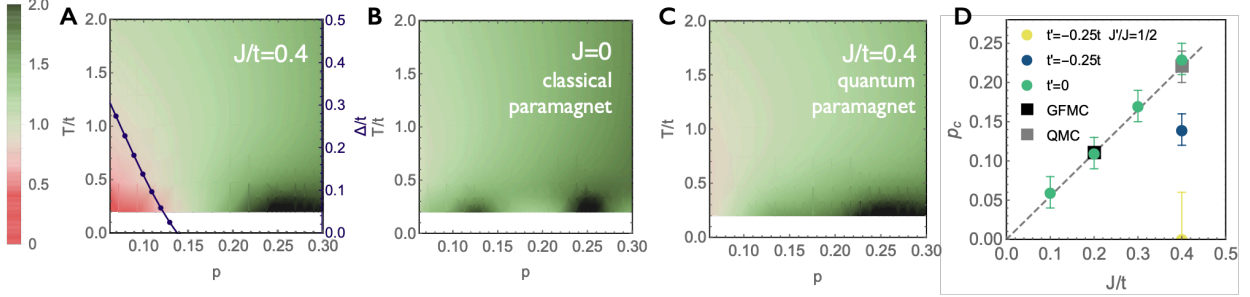


Figure 3: Pervasive Planckian behavior. (A) Maps of the many-body diffusivity in units of the Planckian fundamental value D_{Planck} , as a function of doping p and temperature T , for $J/t = 0.4$ on the square lattice with $t'/t = -0.25$ (here $D_{Planck} = \hbar/m = 1.28ta^2$, determined from the angular-averaged curvature of the band dispersion at half filling). Parameters are $N_s = 16$, $M = 300$ and $N_\phi = 441$. The solid line is the thermal activation gap Δ obtained from exponential fits of $D(T)$ in the range $0.4 < T/t < 0.8$. (B) Same, for $J = 0$ (classical paramagnet); the dark regions indicate commensurability effects at fillings $p = 1/8$ and $p = 1/4$. (C) Same, for $J/t = 0.4$ and a frustrating term $J' = J/2$ (quantum paramagnet). (D) Critical doping obtained from the vanishing of the activation gap in the diffusivity at different values of J and t' . These follow $p_c \approx 0.55J/t$ on the unfrustrated lattice with $t' = 0$ (dashed), in quantitative agreement with Green function Monte Carlo (17) and Quantum Monte Carlo (19) calculations on large clusters. The AF phase is progressively suppressed by magnetic frustration, yielding $p_c \approx 0.14$ for $J/t = 0.4$, $t'/t = -0.25$ ($J'/J = 1/16$) and no ordering for the quantum paramagnet ($J' = J/2$).

Finite hole concentrations and Planckian diffusivity.— Following Refs. (4, 5, 7, 46), we define the many-body diffusion constant D via the Nernst-Einstein relation, $\rho = 1/(e^2\chi_c D)$, where χ_c is the charge compressibility. In correlated systems this type of analysis is considered to be more appropriate than the Drude model, since it does not make any simplifying assumptions on the nature of transport. For a single hole or, more generally, a low-density hole gas, Fermi statistics plays no role and the compressibility takes the classical expression $1/\chi_c = T/p$, recovering the Einstein

relation $\rho = T/(e^2 p D)$, with p the hole concentration. Given that the compressibility already contains an explicit T -linear dependence of thermodynamic origin (detailed balance), strange metal behavior in this limit corresponds to a constant D . Planckian behavior, defined phenomenologically by a slope $\alpha \simeq 1$ in Eq. 1, rigorously translates into a diffusivity taking the fundamental value $D_{\text{Planck}} = \hbar/m$. This coincides with the quantum limit of diffusion proposed in Refs. (47, 48).

For a finite concentration of holes, the diffusivity can be obtained from the separate calculation of ρ and χ_c . Fig. 3A shows a temperature vs hole doping map of the diffusivity in the case with $J/t = 0.4$ and second-neighbor hopping $t'/t = -0.25$ that is relevant to the hole-doped superconducting cuprates. The system features an anti-ferromagnetic quantum critical point (QCP) at $p_c = 0.14 \pm 0.02$, as obtained from the vanishing of the thermal activation gap in $D(T)$ (solid line). Planckian behavior develops from the lowest temperatures in an extended range of dopings $p > p_c$, i.e. wherever AF order is absent.

To disentangle the emergence of Planckian transport from the existence of the QCP, we take advantage of the possibility to tune the magnetic correlations that is enabled by the t-J model. Upon reducing J , the QCP moves to lower dopings (as summarized in panel D) and then disappears altogether, leading to a classical paramagnetic state at $J = 0$ (panel B). Concomitantly, rather than being suppressed, the region of Planckian behavior expands to the entire phase diagram. The same happens upon frustrating the magnetic order by introducing a second-neighbor exchange coupling $J' = J/2$ (panel C), leading to a quantum paramagnetic phase (quantum spin liquid) (49). We conclude that the Planckian behavior found here does not follow from the presence of a QCP, but it is instead pervasive at all the explored doping concentrations as long as AF correlations are suppressed.

$p\rho$ scaling: single-hole nature of strange metal transport.— We close by showing in Fig. 4A the temperature dependence of the resistivity at different doping levels for the experimentally relevant case $J = 0.4$, $t'/t = -0.25$, both in the pristine (dashed) and magnetically frustrated case (solid line). The calculated resistivities in both cases coincide in the disordered phase at $p > p_c$, demonstrating that the presence of J' does not alter the transport properties other than by tuning the magnetic order. We therefore proceed with the analysis of the strange metal in the frustrated, quantum paramagnetic phase at all doping concentrations.

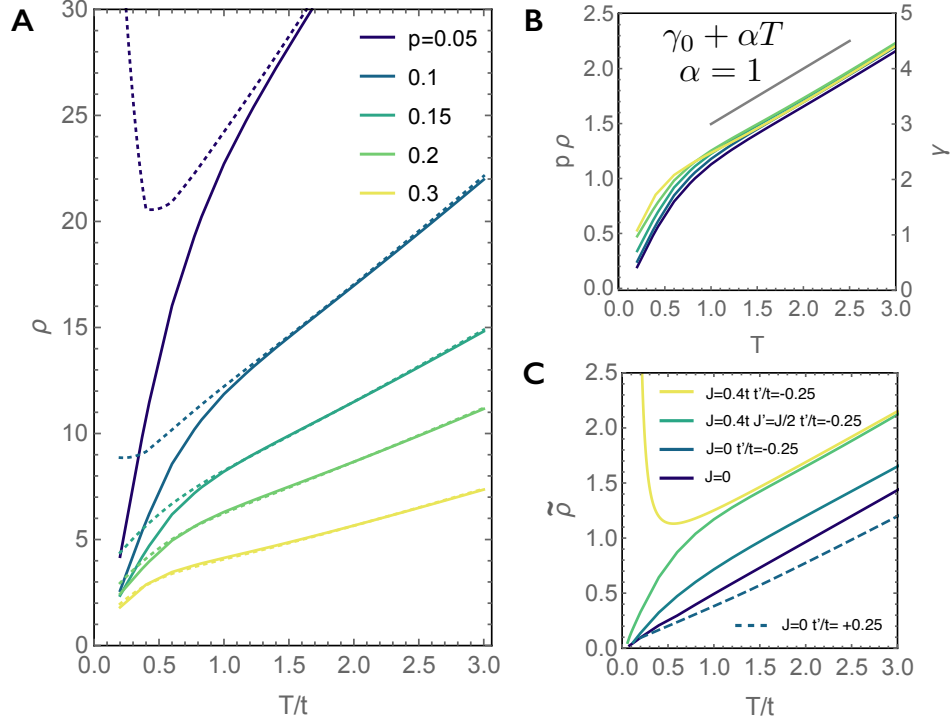


Figure 4: Single-hole nature of strange metal transport. (A) Resistivity at different doping levels for $J = 0.4$ and $t'/t = -0.25$, both in the pristine (dashed) and magnetically frustrated case (solid line, $J'/J = 1/2$). Parameters are the same as in Fig. 3. (B) The data at $J'/J = 1/2$ multiplied by the hole concentration p . (C) Single-hole resistivity $\tilde{\rho}$ calculated in various relevant cases (legends) for $N_s = 18$, $M = 1200$ and $N_\phi = 441$.

Fig. 4B shows that, upon rescaling the resistivity curves by their nominal doping p , these collapse into a "master" curve whose shape is broadly independent on doping, except for a low-temperature offset that moderately increases with doping. This means that the charge carriers move largely independently from one another: the microscopic processes relevant for strange metallicity are already captured at the single-hole level, while mutual hole-hole interactions and Fermi statistics play a minor role on strange metal transport (50). In particular, the two-timescale transport mechanism revealed for a single hole in Figs.1, 2 remains valid at finite hole concentrations.

To a very good approximation, $p\rho$ scaling of the resistivity slope with the hole number is observed experimentally in the cuprates (51). Using typical microscopic parameters $t \approx 400\text{meV}$, $d \approx 6\text{\AA}$, our data at $p = 0.2$ yield low-temperature slopes $d\rho/dT \approx 0.5 - 1\mu\Omega\text{cm}/K$ and room-

temperature resistivities of the order of few hundred $\mu\Omega cm$, in quantitative agreement with the experimental values (14, 51).

We finally illustrate in Fig. 4C the single-hole resistivity for different parameter sets, showing that: (i) In the fully incoherent limit $J = 0$, $t' = 0$, the resistivity is strange and Planckian down to the lowest accessible temperatures. (ii) The slope remains Planckian independent on microscopic parameters at sufficiently high temperature; there the resistivity shows a constant offset that increases with both J and $-t'$ (this includes a negative offset for $t'/t > 0$, representative of electron-doped materials (52, 53)). (iii) Finite J and finite t' partly restore coherence: below a crossover temperature controlled by J and t' quasiparticles are recovered, albeit in an ill-defined form (3); the system enters a low-T strange metal regime where the slope is non-universal (54). For $J/t = 0.4$ and $t'/t = -0.25$ we find $\alpha \simeq 4$, similar to Refs. (3, 5, 6, 55).

Concluding remarks.— Strange metallicity is demonstrated here to arise in strongly correlated systems whenever the hole carriers move in a fluctuating spin environment. The microscopic processes underlying this behavior are already realized for individual holes and they are not crucially affected by mutual hole-hole interactions. As a result, the strange metal behavior found here naturally extends over wide ranges of doping, without requiring the existence of extended quantum criticality (1, 12, 56).

Our calculations show that strong electronic correlations cause a rapid loss of coherence for the carriers as they hop, in line with prevailing theoretical approaches that do not rely on the existence of quasiparticles (9). We demonstrate however the emergence of a second, much slower type of relaxation of the current that sets in at long times, being responsible for both the strange metal resistivity and the non-Drude shape of the optical conductivity.

This long-time anomaly suggests the existence of an additional conducting channel of collective origin, that is not captured by local theories and whose timescale appears to be tightly related to the dynamics of the spin background. In this respect, we note that the presence of current-carrying excitations with a narrow bandwidth, as suggested by their low energy scale, would directly explain the resulting T-linear resistivity (55, 57). At the same time, their characteristic stretched Drude absorption, Eq. (2), seems to accurately describe the optical spectra measured in many correlated electron materials. This scenario would also naturally explain why quenching the spin fluctuations

in the cuprates increases the resistivity and disrupts the T -linear behavior (Ref. (58) and references therein), as this would directly suppress the contribution from the anomalous current carriers.

Possible candidates for these extra carriers could be itinerant spinon excitations, that have been shown to arise in different models for correlated electrons (37, 38, 59), or sound modes that have recently been shown to contribute to heat transport in liquid ^3He (60). In situations where quasiparticles are not completely suppressed, it is conceivable that the same spin fluctuations could also act as scatterers for the original hole carriers, also contributing to the observed strange metal character (61–63). Regardless of these options, the demonstration of unconventional microscopic processes governing charge transport in the normal state makes it appealing to speculate that these may also play a key role in pairing, therefore establishing a microscopic link between strange metal behavior and superconductivity (52, 56).

References and Notes

1. P. W. Phillips, N. E. Hussey, P. Abbamonte, Stranger than metals. *Science* **377** (6602), eabh4273 (2022), doi:10.1126/science.abh4273, <https://www.science.org/doi/abs/10.1126/science.abh4273>.
2. D. N. Basov, T. Timusk, Electrodynamics of high- T_c superconductors. *Rev. Mod. Phys.* **77**, 721–779 (2005), doi:10.1103/RevModPhys.77.721, <https://link.aps.org/doi/10.1103/RevModPhys.77.721>.
3. X. Deng, *et al.*, How Bad Metals Turn Good: Spectroscopic Signatures of Resilient Quasiparticles. *Phys. Rev. Lett.* **110**, 086401 (2013), doi:10.1103/PhysRevLett.110.086401, <https://link.aps.org/doi/10.1103/PhysRevLett.110.086401>.
4. N. Pakhira, R. H. McKenzie, Absence of a quantum limit to charge diffusion in bad metals. *Phys. Rev. B* **91**, 075124 (2015), doi:10.1103/PhysRevB.91.075124.
5. J. Kokalj, Bad-metallic behavior of doped Mott insulators. *Phys. Rev. B* **95**, 041110(R) (2017), doi:10.1103/PhysRevB.95.041110.
6. J. Vučičević, *et al.*, Conductivity in the Square Lattice Hubbard Model at High Temperatures: Importance of Vertex Corrections. *Phys. Rev. Lett* **123**, 036601 (2019), doi:10.1103/PhysRevLett.123.036601.
7. E. W. Huang, R. Sheppard, B. Moritz, T. P. Devereaux, Strange metallicity in the doped Hubbard model. *Science* **366**, 987–990 (2019), doi:10.1126/science.aau7063.
8. W. Wú, X. Wang, A.-M. Tremblay, Non-Fermi liquid phase and linear-in-temperature scattering rate in overdoped two-dimensional Hubbard model. *Proceedings of the National Academy of Sciences* **119** (13), e2115819119 (2022), doi:10.1073/pnas.2115819119, <https://www.pnas.org/doi/abs/10.1073/pnas.2115819119>.
9. D. Chowdhury, A. Georges, O. Parcollet, S. Sachdev, Sachdev-Ye-Kitaev models and beyond: Window into non-Fermi liquids. *Reviews of Modern Physics* **94**, 035004 (2022), doi:<https://doi.org/10.1103/RevModPhys.94.035004>.

10. P. Prelovšek, J. Bonča, *Ground State and Finite Temperature Lanczos Methods* (Springer Berlin Heidelberg, Berlin, Heidelberg), pp. 1–30 (2013), doi:10.1007/978-3-642-35106-8_1, https://doi.org/10.1007/978-3-642-35106-8_1.
11. H. Rammal, A. Ralko, S. Ciuchi, S. Fratini, Transient Localization from the Interaction with Quantum Bosons. *Phys. Rev. Lett.* **132**, 266502 (2024), doi:10.1103/PhysRevLett.132.266502, <https://link.aps.org/doi/10.1103/PhysRevLett.132.266502>.
12. J. Zaanen, Planckian dissipation, minimal viscosity and the transport in cuprate strange metals. *SciPost Phys.* **6**, 061 (2019), doi:10.21468/SciPostPhys.6.5.061, <https://scipost.org/10.21468/SciPostPhys.6.5.061>.
13. J. A. N., B. H. Sakai, R. S. Perry, A. P. Mackenzie, Similarity of Scattering Rates in Metals Showing T-Linear Resistivity. *Science* **339**, 804–807 (2013), doi:10.1126/science.1227612.
14. A. Legros, *et al.*, Universal T-linear Resistivity and Planckian Dissipation in Overdoped Cuprates. *Nature Physics* **15** (2), 142–147 (2019), doi:10.1038/s41567-018-0334-2.
15. J. Zaanen, Why the Temperature Is High. *Nature* **430** (6999), 512–513 (2004), doi:10.1038/430512a.
16. J. Zaanen, Planckian dissipation, minimal viscosity and the transport in cuprate strange metals. *SciPost Phys.* **6**, 061 (2019), doi:10.21468/SciPostPhys.6.5.061, <https://scipost.org/10.21468/SciPostPhys.6.5.061>.
17. M. Lugas, L. Spanu, F. Becca, S. Sorella, Finite compressibility in the low-doping region of the two-dimensional t - J model. *Phys. Rev. B* **74**, 165122 (2006), doi:10.1103/PhysRevB.74.165122, <https://link.aps.org/doi/10.1103/PhysRevB.74.165122>.
18. S. Jiang, D. J. Scalapino, S. R. White, Ground-state phase diagram of the t - J model. *Proceedings of the National Academy of Sciences* **118** (44), e2109978118 (2021), doi:10.1073/pnas.2109978118, <https://www.pnas.org/doi/abs/10.1073/pnas.2109978118>.

19. H. Xu, H. Shi, E. Vitali, M. Qin, S. Zhang, Stripes and spin-density waves in the doped two-dimensional Hubbard model: Ground state phase diagram. *Phys. Rev. Res.* **4**, 013239 (2022), doi:10.1103/PhysRevResearch.4.013239, <https://link.aps.org/doi/10.1103/PhysRevResearch.4.013239>.
20. T. M. Rice, F. C. Zhang, Frequency-dependent conductivity from carriers in Mott insulators. *Phys. Rev. B* **39**, 815–818 (1989), doi:10.1103/PhysRevB.39.815, <https://link.aps.org/doi/10.1103/PhysRevB.39.815>.
21. P. Coleman, *Introduction to Many-Body Physics* (Cambridge university press, Cambridge) (2015).
22. M. Dressel, *Electrodynamics of Solids: Optical Properties of Electrons in Matter* (Cambridge University Press, Cambridge) (2002).
23. D. van der Marel, *et al.*, Quantum Critical Behaviour in a High-Tc Superconductor. *Nature* **425** (6955), 271–274 (2003), doi:10.1038/nature01978.
24. B. Michon, *et al.*, Reconciling Scaling of the Optical Conductivity of Cuprate Superconductors with Planckian Resistivity and Specific Heat. *Nature Communications* **14** (1), 3033 (2023), doi:10.1038/s41467-023-38762-5.
25. S. Paschen, Q. Si, Quantum Phases Driven by Strong Correlations. *Nature Reviews Physics* **3** (1), 9–26 (2020), doi:10.1038/s42254-020-00262-6.
26. Y. S. Lee, *et al.*, Non-Fermi liquid behavior and scaling of the low-frequency suppression in the optical conductivity spectra of CaRuO₃. *Phys. Rev. B* **66**, 041104 (2002), doi:10.1103/PhysRevB.66.041104, <https://link.aps.org/doi/10.1103/PhysRevB.66.041104>.
27. M. M. Zemljič, P. Prelovšek, Resistivity and optical conductivity of cuprates within the t – J model. *Phys. Rev. B* **72**, 075108 (2005), doi:10.1103/PhysRevB.72.075108, <https://link.aps.org/doi/10.1103/PhysRevB.72.075108>.
28. H. Park, K. Haule, C. A. Marianetti, G. Kotliar, Dynamical mean-field theory study of Nagaoka ferromagnetism. *Phys. Rev. B* **77**, 035107 (2008), doi:10.1103/PhysRevB.77.035107, <https://link.aps.org/doi/10.1103/PhysRevB.77.035107>.

29. J. Jaklic, P. Prelovsek, Spectral properties of the planar t-J model. *Phys. Rev. B* **55**, R7307–R7310 (1997), doi:10.1103/PhysRevB.55.R7307, <https://link.aps.org/doi/10.1103/PhysRevB.55.R7307>.
30. L. Prochaska, *et al.*, Singular charge fluctuations at a magnetic quantum critical point. *Science* **367** (6475), 285–288 (2020), doi:10.1126/science.aag1595, <https://www.science.org/doi/abs/10.1126/science.aag1595>.
31. M. A. Quijada, *et al.*, Anisotropy in the ab-plane optical properties of Bi₂Sr₂CaCu₂O₈ single-domain crystals. *Phys. Rev. B* **60**, 14917–14934 (1999), doi:10.1103/PhysRevB.60.14917, <https://link.aps.org/doi/10.1103/PhysRevB.60.14917>.
32. M. Calandra, O. Gunnarsson, Electrical resistivity at large temperatures: Saturation and lack thereof. *Phys Rev. B* **66**, 205105 (2002), doi:10.1103/PhysRevB.66.205105.
33. O. Gunnarsson, M. Calandra, J. E. Han, Colloquium: Saturation of electrical resistivity. *Rev Mod. Phys* **75**, 1085 (2003), doi:10.1103/RevModPhys.75.1085.
34. N. Hussey, K. Takenaka, H. Takagi, Universality of the Mott–Ioffe–Regel limit in metals. *Philos Mag.* **84**, 2847 (2004), doi:10.1080/14786430410001716944.
35. W. F. Brinkman, T. M. Rice, Single-Particle Excitations in Magnetic Insulators. *Phys. Rev. B* **2**, 1324–1338 (1970), doi:10.1103/PhysRevB.2.1324, <https://link.aps.org/doi/10.1103/PhysRevB.2.1324>.
36. R. Strack, D. Vollhardt, Dynamics of a hole in the t-J model with local disorder: Exact results for high dimensions. *Phys. Rev. B* **46**, 13852–13861 (1992), doi:10.1103/PhysRevB.46.13852, <https://link.aps.org/doi/10.1103/PhysRevB.46.13852>.
37. S. A. Trugman, Interaction of holes in a Hubbard antiferromagnet and high-temperature superconductivity. *Phys. Rev. B* **37**, 1597–1603 (1988), doi:10.1103/PhysRevB.37.1597, <https://link.aps.org/doi/10.1103/PhysRevB.37.1597>.
38. F. Grusdt, *et al.*, Parton Theory of Magnetic Polarons: Mesonic Resonances and Signatures in Dynamics. *Phys. Rev. X* **8**, 011046 (2018), doi:10.1103/PhysRevX.8.011046, <https://link.aps.org/doi/10.1103/PhysRevX.8.011046>.

39. A. Vranić, *et al.*, Charge transport in the Hubbard model at high temperatures: Triangular versus square lattice. *Phys. Rev. B* **102**, 115142 (2020), doi:10.1103/PhysRevB.102.115142, <https://link.aps.org/doi/10.1103/PhysRevB.102.115142>.
40. P. Prelovšek, I. Sega, J. Bonča, Scaling of the Magnetic Response in Doped Antiferromagnets. *Phys. Rev. Lett.* **92**, 027002 (2004), doi:10.1103/PhysRevLett.92.027002, <https://link.aps.org/doi/10.1103/PhysRevLett.92.027002>.
41. H. Shackleton, A. Wietek, A. Georges, S. Sachdev, Quantum Phase Transition at Nonzero Doping in a Random t - J Model. *Phys. Rev. Lett.* **126**, 136602 (2021), doi:10.1103/PhysRevLett.126.136602, <https://link.aps.org/doi/10.1103/PhysRevLett.126.136602>.
42. T. Moriya, K. Ueda, Spin fluctuations and high temperature superconductivity. *Advances in Physics* **49** (5), 555–606 (2000), doi:10.1080/000187300412248, <https://doi.org/10.1080/000187300412248>.
43. S. Wakimoto, *et al.*, Direct Relation between the Low-Energy Spin Excitations and Superconductivity of Overdoped High- T_c Superconductors. *Phys. Rev. Lett.* **92**, 217004 (2004), doi:10.1103/PhysRevLett.92.217004, <https://link.aps.org/doi/10.1103/PhysRevLett.92.217004>.
44. M. Mitrano, *et al.*, Anomalous density fluctuations in a strange metal. *Proceedings of the National Academy of Sciences* **115** (21), 5392–5396 (2018), doi:10.1073/pnas.1721495115, <https://www.pnas.org/doi/abs/10.1073/pnas.1721495115>.
45. A. A. Husain, *et al.*, Crossover of Charge Fluctuations across the Strange Metal Phase Diagram. *Phys. Rev. X* **9**, 041062 (2019), doi:10.1103/PhysRevX.9.041062, <https://link.aps.org/doi/10.1103/PhysRevX.9.041062>.
46. S. A. Hartnoll, Theory of Universal Incoherent Metallic Transport. *Nature Physics* **11** (1), 54–61 (2015), doi:10.1038/nphys3174.
47. A. Sommer, M. Ku, G. Roati, M. W. Zwierlein, Universal Spin Transport in a Strongly Interacting Fermi Gas. *Nature* **472** (7342), 201–204 (2011), doi:10.1038/nature09989.

48. A. B. Bardoun, *et al.*, Transverse Demagnetization Dynamics of a Unitary Fermi Gas. *Science* **344** (6185), 722–724 (2014), doi:10.1126/science.1247425, <https://www.science.org/doi/abs/10.1126/science.1247425>.
49. H.-C. Jiang, H. Yao, L. Balents, Spin liquid ground state of the spin- $\frac{1}{2}$ square J_1 - J_2 Heisenberg model. *Phys. Rev. B* **86**, 024424 (2012), doi:10.1103/PhysRevB.86.024424, <https://link.aps.org/doi/10.1103/PhysRevB.86.024424>.
50. K. Wu, Z. Y. Weng, J. Zaanen, Sign structure of the t - J model. *Phys. Rev. B* **77**, 155102 (2008), doi:10.1103/PhysRevB.77.155102, <https://link.aps.org/doi/10.1103/PhysRevB.77.155102>.
51. Y. Ando, S. Komiyama, K. Segawa, S. Ono, Y. Kurita, Electronic Phase Diagram of High- T_c Cuprate Superconductors from a Mapping of the In-Plane Resistivity Curvature. *Phys. Rev. Lett.* **93**, 267001 (2004), doi:10.1103/PhysRevLett.93.267001, <https://link.aps.org/doi/10.1103/PhysRevLett.93.267001>.
52. K. Jin, N. P. Butch, K. Kirshenbaum, J. Paglione, R. L. Greene, Link between Spin Fluctuations and Electron Pairing in Copper Oxide Superconductors. *Nature* **476** (7358), 73–75 (2011), doi:10.1038/nature10308.
53. N. R. Poniatowski, T. Sarkar, R. P. S. M. Lobo, S. Das Sarma, R. L. Greene, Counterexample to the conjectured Planckian bound on transport. *Phys. Rev. B* **104**, 235138 (2021), doi:10.1103/PhysRevB.104.235138, <https://link.aps.org/doi/10.1103/PhysRevB.104.235138>.
54. We note that the low-temperature slope in Fig. 4B is considerably larger than the $\alpha \simeq 1$ obtained in the large-T limit, as also found in the Hubbard model (3, 5, 6, 55). When the resistivities (both measured and calculated, as these coincide) are converted into scattering rates via the Drude analysis, a Planckian slope α of order 1 is however accidentally recovered around $p = 0.2$ when using the total number of electrons $1 - p$ instead of the hole number p (13, 14), provided that the renormalized hole mass $m^*/m \simeq 7$ (64) is used instead of the bare band mass. For the reasons explained in the preceding paragraphs, this accidental agreement should not be taken as an indication of the validity of the Drude model.

55. S. Ciuchi, S. Fratini, Strange metal behavior from incoherent carriers scattered by local moments. *Phys. Rev. B* **108**, 235173 (2023), doi:10.1103/PhysRevB.108.235173, <https://link.aps.org/doi/10.1103/PhysRevB.108.235173>.
56. N. Hussey, High-temperature superconductivity and strange metallicity: Simple observations with (possibly) profound implications. *Physica C: Superconductivity and its Applications* **614**, 1354362 (2023), doi:<https://doi.org/10.1016/j.physc.2023.1354362>, <https://www.sciencedirect.com/science/article/pii/S0921453423001533>.
57. N. H. Lindner, A. Auerbach, Conductivity of hard core bosons: A paradigm of a bad metal. *Phys. Rev. B* **81**, 054512 (2010), doi:10.1103/PhysRevB.81.054512, <https://link.aps.org/doi/10.1103/PhysRevB.81.054512>.
58. I. Vinograd, *et al.*, Competition between spin ordering and superconductivity near the pseudogap boundary in $\text{La}_{2-x}\text{Sr}_x\text{CuO}_4$: Insights from NMR. *Phys. Rev. B* **106**, 054522 (2022), doi:10.1103/PhysRevB.106.054522, <https://link.aps.org/doi/10.1103/PhysRevB.106.054522>.
59. T. Senthil, S. Sachdev, M. Vojta, Fractionalized Fermi Liquids. *Phys. Rev. Lett.* **90**, 216403 (2003), doi:10.1103/PhysRevLett.90.216403, <https://link.aps.org/doi/10.1103/PhysRevLett.90.216403>.
60. K. Behnia, K. Trachenko, How Heat Propagates in Liquid ^3He . *Nature Communications* **15** (1), 1771 (2024), doi:10.1038/s41467-024-46079-0.
61. T. Moriya, Y. Takahashi, K. Ueda, Antiferromagnetic Spin Fluctuations and Superconductivity in Two-Dimensional Metals -A Possible Model for High T_c Oxides. *Journal of the Physical Society of Japan* **59** (8), 2905–2915 (1990), doi:10.1143/JPSJ.59.2905, <https://doi.org/10.1143/JPSJ.59.2905>.
62. S. Caprara, C. D. Castro, G. Mirarchi, G. Seibold, M. Grilli, Dissipation-driven strange metal behavior. *Communications Physics* **5** (1), 10 (2022), doi:10.1038/s42005-021-00786-y, <https://doi.org/10.1038/s42005-021-00786-y>.

63. A. A. Patel, P. Lunts, S. Sachdev, Localization of overdamped bosonic modes and transport in strange metals. *Proceedings of the National Academy of Sciences* **121** (14), e2402052121 (2024), doi:10.1073/pnas.2402052121, <https://www.pnas.org/doi/abs/10.1073/pnas.2402052121>.
64. D. Poilblanc, E. Dagotto, Optical mass in the t-J model. *Phys. Rev. B* **44**, 466–469 (1991), doi:10.1103/PhysRevB.44.466, <https://link.aps.org/doi/10.1103/PhysRevB.44.466>.

Acknowledgments

S.F. acknowledges kind hospitality from the Biblioteca de Catalunya and Jozef Stefan Institute, where this manuscript was written, and useful discussions with K. Behnia, M. Dressel, A. Georges, T. Giamarchi, D. Golez, M.-H. Julien, J. Kokalj, D. LeBoeuf, D. van der Marel, L. de' Medici, J. Mravlje, P. Prelovšek, L. Rademaker, H. Rammal, C. Swickard. S.F. is particularly grateful to M.-H. Julien for suggesting the study of the frustrated quantum paramagnet, and to M. Dressel for recommending the denomination "stretched Drude peak" for the functional form of the low-energy optical absorption proposed in this work. S.C. acknowledges useful discussions with S. Caprara. S.C. acknowledges funding from NextGenerationEU National Innovation Ecosystem Grant No. ECS00000041- VITALITY-CUP E13C22001060006.

Author contributions: S.F. had the initial idea, led the project, devised the methodology, wrote the FTLM code and the manuscript. A.R. wrote the FTLM code and helped with the interpretation of the results. SC helped with the interpretation of the results.